

Cooperative Transportation of Loads with UAVs

Tiago Marquês Bacelar¹

tiago.bacelar@tecnico.ulisboa.pt

¹ Instituto Superior Técnico, Universidade de Lisboa, Portugal

June 2019

Abstract—This thesis presents a methodology for cooperative load transportation by two quadrotors, given the state variables estimates, based on measurements from motion sensors installed onboard. The control and estimation solutions were required to ensure the stability of the system while guarantying null steady-state position and estimation errors. The vertical velocity has to be estimated since there is no sensor usually onboard the quadrotors capable of providing this measurement directly.

Further, in order to turn the system independent of a motion tracking system to provide estimates of the relative position between the multiple UAVs, the UAVs front camera is meant to be used in order to provide these estimates. Therefore, the relative velocity between the UAVs can be estimated upon these measurements.

The proposed solutions are presented based on linear control and estimation methods. These solutions include classical and optimal control and estimation theory. The controllers and estimators resort to linear and optimal control techniques, as the Linear Quadratic Regulators (LQRs) and Kalman filters.

The proposed control system is validated both in simulation and experimentally, resorting to a commercially available quadrotor equipped with an Inertial Measurement Unit (IMU), an ultrasound height sensor, vertical and frontal cameras, among other sensors. The simulation environment models the noise present in the measurements provided by the sensors, as Gaussian white-noise for the experimental implementation of the control system proposed.

I. INTRODUCTION

In the last decades, the interest in Unmanned Aerial Vehicles (UAV) has increased due to the development and wide commercialization of these type of vehicles. They can operate in highly constrained environments with multiple obstacles, hostiles and impossible to reach by humans. For these reasons they became very useful for a wide range of civil and military applications, such as environment monitoring, surveillance, search and rescue missions and transportation of cargo. One of the major limitations on the available models is in terms of payload carrying capacity, being required the cooperation of several of these vehicles for several applications.

The manipulation of a towed cable system resorting to a aerial vehicle has been studied in [1]. A control method for the transportation of tethered known loads with a single quadrotor is proposed in [2], resorting to a Mixed Integer Quadratic Program focusing on aggressive maneuvering. Methods to tackle applications where the load is unknown are proposed, both for the estimation and the control of the height of a single quadrotor in [3]. Cooperative methods for cooperative manipulation and transportation using multiple aerial vehicles based on quasi-static models are proposed in [4], focusing on the position and orientation control of a payload with six

degrees of freedom. The same problem is addressed in [5], studying the dynamics of cooperative manipulation resorting to a complete dynamical model for the cases when the payload is considered to be a point load, and a three-dimensional rigid body.

In this thesis, a method for cooperative load transportation is proposed. It is assumed that the length of the load is greater than the distance between both UAVs as shown in Fig. 2, thus a configuration is envisioned where longitudinal forces are small and thus will be neglected. Moreover, the air flow cross disturbance can also be neglected due to the abovementioned geometry.

A position control loop using LQRs is proposed for the rear UAV, and for estimation a linear Kalman filter is considered. The motion sensors used are a gyroscope, a magnetometer, a ultrasound sensor and a downward pointing camera for optical flow computation proposes, all usually available on-board a quadrotor. The on board Inertial Measurement Unit (IMU) allows the measurement and estimation of the height, attitude angles, accelerations, angular, and ground velocities.

This paper is organized as follows: the problem addressed in this paper is described in Section II. The physical model considered is presented in Section III. The solution for the control problem is proposed in Section IV, and the solution for estimation is presented in Section V. In Section VI simulation results are presented and discussed. In Section VII experimental results are presented and analyzed. Finally, some concluding remarks are presented in Section VIII.

II. PROBLEM STATEMENT

For the control systems design regarding the cooperative transportation of loads with two quadrotors, the controllability property plays a crucial role, such as stabilization of unstable systems, alongside the observability property which measures how well system's internal states can be inferred from knowledge of its own external outputs. The controllability and observability of a system are mathematical duals. A more in depth survey can be found in [6]. For the envisioned solution it is mandatory that both properties are verified. The main goal is to control the quadrotors 3D inertial position and orientation with respect to a reference North-East-Down (NED) frame. The two quadrotors to be considered are denoted as front UAV and rear UAV, which configuration is presented in Fig. 2.

Given the difficulties proving the system controllability and observability when considering the two UAVs as an ensemble with one common state space, a different approach

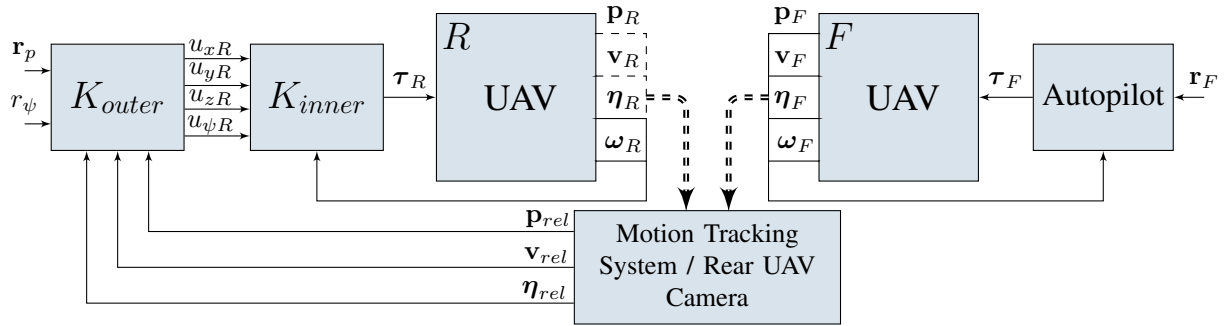


Fig. 1: Control System Architecture

is exploited. In this approach is taken into consideration the following assumptions:

- The front UAV is piloted by an operator
- The relative position and orientation between both UAVs is computed with respect to the rear UAV
- The effect of the load on the UAVs dynamics are neglected

In regard to control the front UAV position and orientation, externally to the rear UAV, a control system for the front UAV must be designed. Under these circumstances the front UAV will be able to maintain its position over a desired location, and therefore stably follow a designed trajectory autonomously, which is required to the solution proposed. The control systems are designed resorting to optimal control techniques, namely, linear quadratic regulators, which requires full state feedback. In order to reduce the noise impact present in the system measurements, and to ensure the full state feedback, discrete linear Kalman Filters will be designed.

The relative position between both UAVs is the primary state to control since the system's stability relies on this. Poor control of the relative position may lead to undesirable oscillations and twisting forces which can turn the system unstable resulting in the crash of both drones. Ideally, the rear UAVs frontal camera would be used to estimate the relative position, velocity and orientation with respect to the rear UAV body-fixed frame. The relative velocity can be computed resorting to optical flow techniques or resorting to a complementary filter upon the relative position estimation. However, in order to first evaluate the feasibility of the proposed control system, a precision motion capture and 3D positioning tracking system is used to perform the estimation, namely, Qualisys motion capture system [7].

Then, concerning the estimation of the relative velocities upon the position measurements, will be designed and implemented complementary filters. Both UAVs have a slight delay between them since the rear UAV waits for detection of an actuation of the front UAV to respond. Thus, aggressive responses from the front UAV can lead to an increased error in the relative position desired to maintain between them, and then eventually escape to out of the rear UAV camera measurements range. Therefore, low pass filters will be designed implemented on the front UAV, in order to reduce

the control system bandwidth attenuating the high frequencies and increase the control system robustness.

Lastly, the frontal camera of the front UAV will be used in order to estimate the relative position and orientation between both UAVs expressed in the body-fixed frame of the rear UAV. In this experiment, the system will be independent, since the sensors onboard will provide all the estimations required for the latter control system proposed.

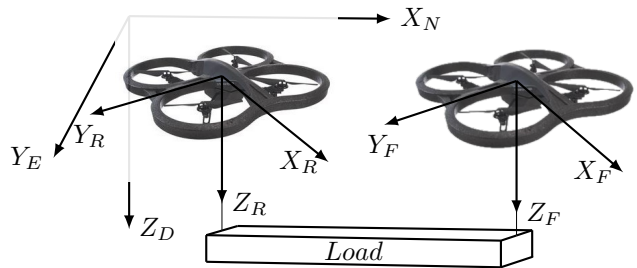


Fig. 2: Rear and Front UAV Configuration

III. PHYSICAL MODEL

The physical model is obtained resorting to the North-East-Down (NED) inertial frame and to the quadrotor body-fixed frame. A more detailed description of the quadrotor physical model without a load can be found in [8]. Let $\mathbf{v} = (u, v, w)^T$ represent the linear velocity vector in the ENU inertial frame, $\boldsymbol{\eta} = (\phi, \theta, \psi)^T$ denote the orientation vector of the body-fixed frame with respect to the inertial frame in terms of Euler angles, and the body-axis angular rate vector be described by $\boldsymbol{\Omega} = (p, q, r)^T$.

The position behaviour where the influence of the Coriolis effects and the provided angular moments are defined in the following equation

$$m\dot{\mathbf{v}} = m\mathbf{g} + \mathbf{R}_B^T \mathbf{F}^B - \mathbf{v} \times \boldsymbol{\omega} \quad (1)$$

where $\mathbf{g} = (0, 0, g)^T$ is the gravity vector with respect to the inertial frame, g is the gravitational acceleration, \mathbf{R}_B^T is the rotation matrix responsible for rotate the quadrotor body-fixed frame into the NED inertial frame is presented in (2). \mathbf{F}^B corresponds to the total force applied in the quadrotor in terms of a vector with respect to the body-fixed frame presented in (3). Here \mathbf{f}^B is the actuation force vector, \mathbf{g}_T^B is the rotation

matrix that rotates the NED inertial frame into the body-fixed frame, and \mathbf{t} is the tension force applied to the UAV which is assumed to be approximately null.

$$\mathbf{R}_B^I(\boldsymbol{\eta}) = \begin{bmatrix} c\psi c\theta & -c\theta s\psi & s\theta \\ c\phi s\psi - c\psi s\theta s\phi & c\psi c\phi + s\psi s\theta s\phi & c\theta s\phi \\ -s\psi s\phi - c\psi c\phi s\theta & c\theta s\psi s\theta - c\psi s\phi & c\theta c\phi \end{bmatrix} \quad (2)$$

$$\mathbf{F}^B = \mathbf{f}^B + \mathbf{R}_T^B(\mathbf{v} \times \boldsymbol{\omega}) + \mathbf{t} \quad (3)$$

Substituting (3) in (1), yields

$$m\dot{\mathbf{v}} = m\mathbf{g} + \mathbf{f}^T \quad (4)$$

where $\mathbf{f}^T = \mathbf{R}_B^T \mathbf{f}^B$.

The angular behaviour which takes into consideration Coriolis effects influence is presented in the following equation

$$\mathbf{J}\dot{\boldsymbol{\Omega}} = -\boldsymbol{\Omega} \times \mathbf{J}\boldsymbol{\Omega} + \boldsymbol{\tau} \quad (5)$$

where \mathbf{J} is the inertia matrix and $\boldsymbol{\tau}$ is the torque vector that results from a combination of differences between the thrust forces generated by each of the four rotors.

IV. CONTROL

In this Section the control solution is discussed. First the LQR is introduced followed by the controllers design for both UAVs.

A. Linear Quadratic Regulator

Consider the following linear time-invariant (LTI) dynamical system presented in (6). Here the vector \mathbf{x} is the $n \times 1$ state vector, and the $m \times 1$ vector \mathbf{u} is the control input. The control input is defined to be state feedbacks of the form is given in (7), where \mathbf{K} is the state feedback control gain matrix that minimizes the quadratic cost function presented in (8).

$$\dot{\mathbf{x}} = \mathbf{A}\mathbf{x} + \mathbf{B}\mathbf{u} \quad (6)$$

$$\mathbf{u} = -\mathbf{K}\mathbf{x} \quad (7)$$

$$J = \int_0^\infty (\mathbf{x}^T \mathbf{Q}\mathbf{x} + \mathbf{u}^T \mathbf{R}\mathbf{u}) dt \quad (8)$$

In this performance index, the matrices \mathbf{Q} and \mathbf{R} determine the relative importance of the energy associated to the states or to the control action, respectively. The control vector $\mathbf{u}(t)$ is assumed to be unconstrained. The infinite time quadratic optimal control problem relies on the minimization of the cost function J . The optimal gain matrix for the infinite time quadratic optimal control problem is linear and is given in (9). The matrix \mathbf{P} in (9) must satisfy the algebraic Riccati equation presented in (10).

$$\mathbf{K} = \mathbf{R}^{-1} \mathbf{B}^T \mathbf{P} \quad (9)$$

$$\mathbf{A}^T \mathbf{P} + \mathbf{P}\mathbf{A} - \mathbf{P}\mathbf{B}\mathbf{R}^{-1} \mathbf{B}^T \mathbf{P} + \mathbf{Q} = 0 \quad (10)$$

The optimal state feedback control gain matrix \mathbf{K} is given by substituting the matrix \mathbf{P} obtained by solving the (10) into (9).

B. Controllers Design

This subsection presents the position and orientation control design for both UAVs. The position control is responsible for maintain the UAV over a desired position.

The position controller for both UAVs is designed and implemented of over an internal attitude control. Since this attitude inner loop is assumed to be significantly faster than the outer loop, the system's planar motion can be interpreted as a dominantly second-order system.

The UAVs are controlled by giving the following set of inputs:

- u_x front/back bending angle, assuming negative values bending forward and zero on the horizontal plane
- u_y left/right bending angle, assuming negative values bending leftward
- u_z vertical speed
- u_ψ angular speed around the yaw axis

In order to allow the choice between smooth and dynamic moves, this input arguments are not directly the control parameter values, but a percentage of the maximum corresponding values as set in the embedded attitude control parameters. Therefore, the input signals must be floating values within $[-1.0, 1.0]$. The internal attitude control loop is responsible for translate the set of inputs mentioned above to individual motor speeds.

In order to distinguish both UAVs, index subscripts R and F are used to denote the rear and front UAV, respectively.

1) Front UAV:

For the front UAV, the objective is the design of an autopilot external control loop by giving as input the desired inertial position and orientation values, denoted as \mathbf{r}_F , in order to maintain the UAV over the desired position. This autopilot is responsible for translate the input references into thrust forces to be generated by each rotor, resorting the inertial position, body-fixed frame velocities, Euler angles and rates, measurements based on sensors installed on board.

2) Rear UAV:

The control system for the rear UAV could also be a commercially available autopilot, however controllability would be compromised. Thus, for the rear UAV, the objective is the design of an external control loop by giving the desired relative position and orientation values between both UAVs in respect to the rear UAV body-fixed frame, in order to maintain the UAV over the desired relative position while orientated with respect to the desired relative orientation.

The full dynamical model of the configuration proposed is derived based on the Lagrangian mechanics, modeling the payload was a 6 degree of freedom rigid body and the cables which attach the payload to the UAVs as mass-less rigid links. In other words, the cables are assumed to be always stretched. The controllers proposed are designed based on a linearization of these dynamics under some simplifying assumptions of this full dynamical model. Since it is meant to control the rear UAV relative position and orientation with respect to its body-fixed frame, and assuming that both UAVs share the same dynamics, the dynamical system upon which it is meant to

base the control design can be represented by the following equations:

$$\begin{aligned} m\dot{\mathbf{v}}_{rel} &= \mathbf{f}_F^T - \mathbf{f}_R^T \\ \dot{\mathbf{p}}_{rel} &= \mathbf{v}_{rel} \\ \mathbf{z} &= \mathbf{C}\mathbf{p}_{rel} \end{aligned} \quad (11)$$

where $\mathbf{v}_{rel} = \mathbf{v}_F - \mathbf{v}_R$, $\mathbf{p}_{rel} = \mathbf{p}_F - \mathbf{p}_R$ and \mathbf{C} is the output matrix. Since \mathbf{f}_F^T is the front UAV actuation force vector, \mathbf{f}_F^T is assumed as an external disturbance. The relative attitude angles are depicted as $\boldsymbol{\eta}_{rel}$.

An external control loop is designed taking into consideration that \mathbf{p}_{rel} , \mathbf{v}_{rel} and $\boldsymbol{\eta}_{rel}$, can be measured resorting to the motion tracking system. The external control loop expects a reference relative position and orientation, and combines these references with the sensors measurements in order to obtain the desired roll, pitch, angular velocity around the yaw axis and vertical velocity, which are the attitude inner loop set of inputs. The inner attitude control loop is responsible for prescribing these inputs into individual rotors velocities. The control System architecture is depicted in Fig. 1.

Since the relative position control design is based on the rear UAV body-fixed frame, the relative position tracking errors with respect to the NED frame are presented in the following equation:

$$\mathbf{e}_p = \mathbf{r}_p - \mathbf{R}_T^B \mathbf{p}_{rel} \quad (12)$$

where $\mathbf{r}_p = (x_d, y_d, z_d)^T$ is the desired relative position reference vector between both UAVs in respect to the rear UAV body-fixed frame, and \mathbf{R}_T^B is the rotation matrix that describes the rotation of the NED frame into the rear UAV body-fixed frame.

Therefore, the inner control loop input vector is computed as follows:

$$\begin{bmatrix} u_x \\ u_y \\ u_z \end{bmatrix} = \begin{bmatrix} K_x & 0 & 0 \\ 0 & K_y & 0 \\ 0 & 0 & K_z \end{bmatrix} \mathbf{e}_p - \mathbf{K}_{xyz} \begin{bmatrix} \mathbf{v}_{rel} \\ \boldsymbol{\eta}_{rel} \\ \zeta \end{bmatrix} \quad (13)$$

where K_x , K_y and K_z are the position optimal gains, and \mathbf{K}_{xyz} is the optimal gain matrix suppressing the gains regarding the position position states.

Resorting to relative position in respect to the NED frame, the relative yaw orientation from the rear to the front UAV can be computed as:

$$\psi_r = \psi_R + \tan^{-1} \left(\frac{y_F - y_R}{x_F - x_R} \right) \quad (14)$$

Therefore, the orientation input control vector for the rear UAV is presented in (15).

$$u_\psi = K_\psi (\psi_r - \psi_r) \quad (15)$$

V. ESTIMATION

In this Section the discrete linear Kalman filter is introduced, followed by the vertical velocity estimation.

A. Linear Kalman Filter

This Section presents the discrete Kalman filter derived using parameter optimization without making any gaussian assumptions on the probability density function, resorting to [9] for the continuous-time case. Consider the following discrete LTI dynamical system:

$$\begin{aligned} \mathbf{x}_{k+1} &= \mathbf{F}\mathbf{x}_k + \mathbf{G}\mathbf{u}_k + \mathbf{w}_k \\ \mathbf{z}_k &= \mathbf{H}\mathbf{x}_k + \mathbf{v}_k \end{aligned} \quad (16)$$

where the vector \mathbf{x}_k is the $n \times 1$ state vector, the $m \times 1$ \mathbf{u}_k is the control input and the $r \times 1$ \mathbf{z}_k is the output vector. \mathbf{w}_k is the zero-mean white Gaussian process noise vector that conveys the system error sources, and \mathbf{v}_k is the zero-mean white Gaussian process noise vector that represents the measurement error sources. Both noise vectors are mutually independent sequences of zero mean white Gaussian noise, which covariance matrix is presented in (17). Here \mathbf{Q}^K is a positive-definite (or positive-semidefinite) Hermitian or real symmetric matrix and \mathbf{R}^K is a positive-definite Hermitian or real symmetric matrix.

$$E \left(\begin{bmatrix} \mathbf{w}_k \\ \mathbf{v}_k \end{bmatrix} \begin{bmatrix} \mathbf{w}_k^T & \mathbf{v}_k^T \end{bmatrix} \right) = \begin{bmatrix} \mathbf{Q}^K & \mathbf{0} \\ \mathbf{0} & \mathbf{R}^K \end{bmatrix} \quad (17)$$

1) Predict Phase:

The *a priori* state estimate and the *a priori* error covariance are computed in (18) and (19), respectively.

$$\hat{\mathbf{x}}_{k+1|k} = \mathbf{F}\hat{\mathbf{x}}_{k|k} + \mathbf{G}\mathbf{u}_k \quad (18)$$

$$\mathbf{P}_{k+1|k} = \mathbf{F}\mathbf{P}_{k|k}\mathbf{F}^T + \mathbf{Q}^K \quad (19)$$

2) Update Phase:

The Kalman gain matrix is computed in (20). The *a posteriori* estimation and the *a posteriori* estimate covariance are presented in (21) and (22).

$$\mathbf{K}_k = \mathbf{P}_{k|k-1}\mathbf{H}^T(\mathbf{H}\mathbf{P}_{k|k-1}\mathbf{H}^T + \mathbf{R}^K)^{-1} \quad (20)$$

$$\hat{\mathbf{x}}_{k|k} = \hat{\mathbf{x}}_{k|k-1} + \mathbf{K}_k(\mathbf{z}_k - \mathbf{H}\hat{\mathbf{x}}_{k|k-1}) \quad (21)$$

$$\mathbf{P}_{k|k} = (\mathbf{I}_n - \mathbf{K}_k\mathbf{H})\mathbf{P}_{k|k-1} \quad (22)$$

B. Velocities Estimation

In order to estimate the vertical and ground velocity upon position measurements, a complementary filter is designed regarding to the Kalman filter theory. For this purpose is considered the discrete filter's state-space representation presented in (23).

$$\mathbf{F} = \begin{bmatrix} 1 & \Delta \\ 0 & 1 \end{bmatrix}, \quad \mathbf{H} = \begin{bmatrix} 1 & 0 \end{bmatrix}, \quad \mathbf{G} = \begin{bmatrix} 0 \\ 1 \end{bmatrix} \quad (23)$$

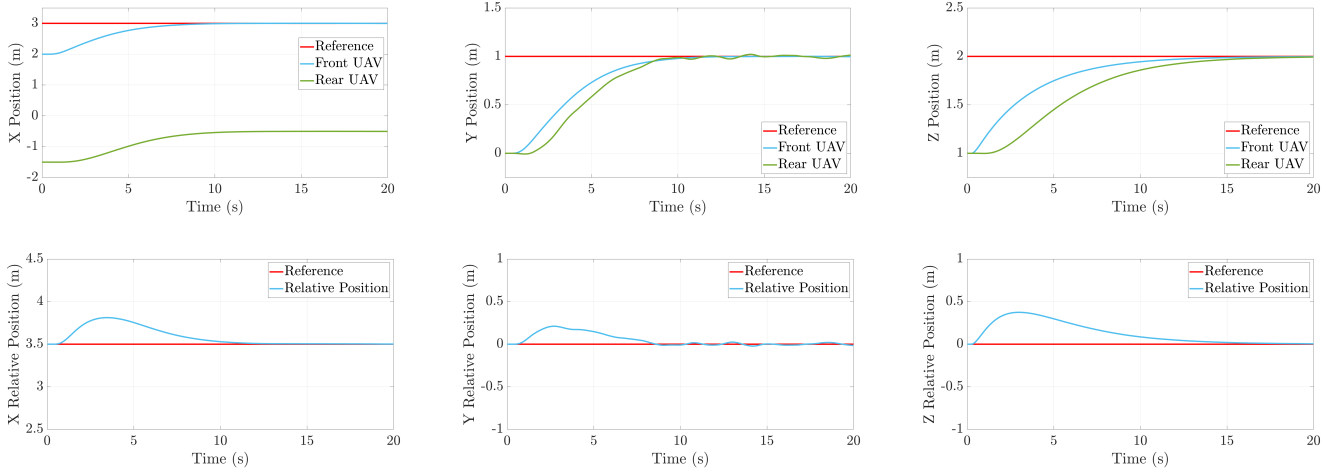


Fig. 3: Simulation results. From left to right, top to bottom: (a) X Position, (B) Y Position, (C) Z Position, (D) X Relative Position, (E) Y Relative Position, (F) Z Relative Position

C. Position and Orientation Filter (Frontal Camera)

In this section is briefly presented the position and orientation filter designed by the colleague João Madeiras in [10], used for the estimation of the relative position, velocity, and orientation between both UAVs. This filter presents a Visual-Aided landmark positioning system aided IMU using complementary filters. Here, an innovative alluring method is presented using color feature recognition for landmark tracking concerning the computation of the position and attitude relative to a target via the algebraic Robust solution to the Perspective-n-Point RPnP. The measurements obtained are then fused with the optical flow measurements available onboard the UAV.

The following state-space representation describes the position kinematics using the optical flow measurements

$$\begin{bmatrix} \mathbf{x} \\ \mathbf{b}_v \end{bmatrix}_{k+1} = \begin{bmatrix} \mathbf{I} & -\Delta\mathbf{R}_k \\ \mathbf{0} & \mathbf{I} \end{bmatrix} \begin{bmatrix} \mathbf{x} \\ \mathbf{b}_v \end{bmatrix}_k + \begin{bmatrix} \Delta\mathbf{R}_k \\ \mathbf{0} \end{bmatrix} \mathbf{v}_k + \begin{bmatrix} \Delta\mathbf{R}_k & \mathbf{0} \\ \mathbf{0} & \mathbf{I} \end{bmatrix} \begin{bmatrix} \mathbf{n}_p \\ \mathbf{n}_b \end{bmatrix}_k \quad (24)$$

where \mathbf{x} and \mathbf{v} are the position and velocity in the chosen inertial frame and fixed-body frame coordinates, respectively. \mathbf{R} denotes the rotational matrix from the body-fixed frame $\{\mathcal{B}\}$ to the inertial frame $\{\mathcal{I}\}$ placed at the landmarks plane. \mathbf{b}_v represents the velocity bias. \mathbf{n}_p and \mathbf{n}_b denotes zero-mean Gaussian white-noise that accounts for disturbances in the position and in the velocity bias, respectively.

The position observer is given by the following nonlinear feedback system

$$\begin{bmatrix} \hat{\mathbf{x}} \\ \hat{\mathbf{b}}_v \end{bmatrix}_{k+1} = \begin{bmatrix} \mathbf{I} & -\Delta\mathbf{R}_k \\ \mathbf{0} & \mathbf{I} \end{bmatrix} \begin{bmatrix} \hat{\mathbf{x}} \\ \hat{\mathbf{b}}_v \end{bmatrix}_k + \begin{bmatrix} \Delta\mathbf{R}_k \\ \mathbf{0} \end{bmatrix} \mathbf{v}_k + \begin{bmatrix} \mathbf{R}_k (\mathbf{K}_{1x} - \mathbf{I}) + \mathbf{R}_{k-1} \\ \mathbf{K}_{2b_v} \end{bmatrix} \mathbf{R}_{k-1}^T (\mathbf{x}_k - \hat{\mathbf{x}}_k) \quad (25)$$

where \mathbf{K}_{1x} and \mathbf{K}_{2b_v} are the Kalman gains computed for the system presented in equation 24 with $\mathbf{R}_k = \mathbf{I}$.

The measurement of the position filter presented in equation 25 is given by a landmark target consisting of 6 markers. The landmarks are placed in the same plane, and a YCbCr color segmentation via Mahalanobis distance is used for the segmentation of the markers from the background. After segmenting the markers, the respective centroids are computed and, the RPnP technique is used, providing the position and orientation of the camera relative to the landmark target plane. Only the position in X and Y-axis and the yaw angle is used as a measurement.

VI. SIMULATION RESULTS

In this section, the simulation results are presented and analyzed.

A. Simulation environment

In order to validate the feasibility of the control system designed a simulation environment was prepared. For this propose is used the dynamical models provided in [11]. The use of this dynamical models is justified by the commercially available quadrotor in use. Firstly, is presented the simulation results regarding the position controller's design for both UAVs based on unit step responses. Then, is presented the simulation results regarding the new control system with the implementation from the intermediary filters.

The selected sample time for this environment is 0.065 seconds.

B. Step Analysis

The LQR gains regarding the X and Y position were calculated using a $\mathbf{Q} = \text{diag}(3, 1, 1, 0)$, and for Z position using a $\mathbf{Q} = \text{diag}(3, 1)$. For the front UAV, the weighting matrices \mathbf{R} regarding XYZ are 270, 100, and 20, respectively. Analogously, the weighting matrices \mathbf{R} regarding the rear UAV controller design are 270, 30, and 10.

The simulation results regarding the consequent unit step responses are presented in Fig. 3. Here, the unit step responses for the XYZ directions regarding the front UAV present a settling time (5%) is at 7.9, 8.4 and 9.5 seconds, respectively,

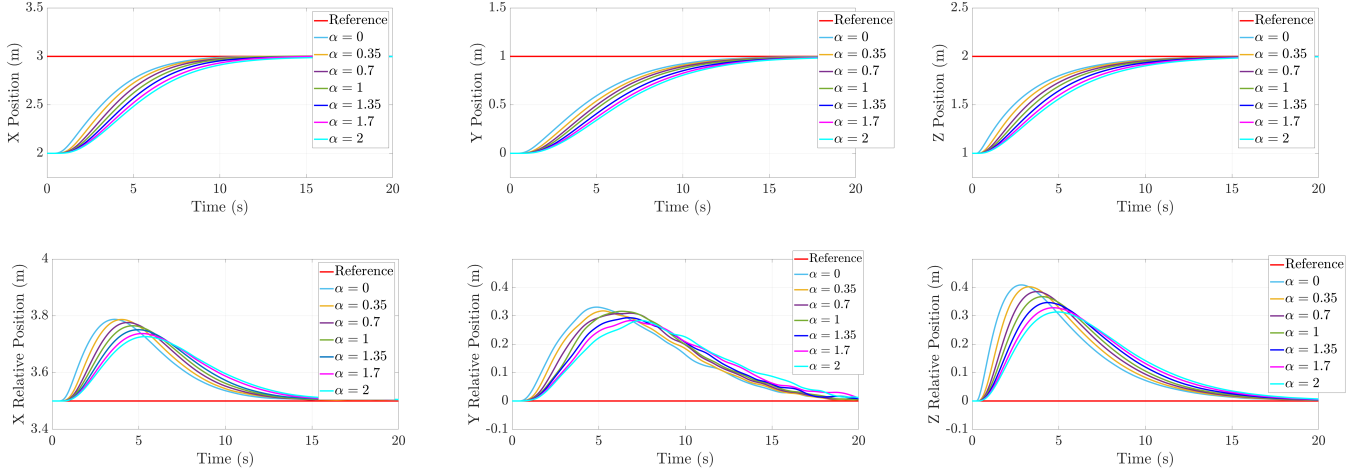


Fig. 4: Simulation results concerning the implementation of the intermediary filters. From left to right, top to bottom: (a) Front UAV X Position, (B) Front UAV Y Position, (C) Front UAV Y Position, (D) X Relative Position, (E) Y Relative Position, (F) Z Relative Position

and it is duly noted an absence of overshoot. The relative position between both UAVs along the XYZ directions settles at 8.8, 7.2 and 5.7 seconds, respectively. The maximum relative position errors between both UAVs along the XYZ directions is 31, 20, 26 centimeters, respectively.

C. Intermediary Filters

In this subsection is addressed the low pass filters tune analyzing the effect of the time constant α variation on the system dynamics. Since it is meant to estimate the relative velocities upon the relative position when using the rear UAV camera to perform this estimation. Complementary filters are designed and implement concerning the estimations of the relative velocities. The LQR gains regarding the X, Y and Z position were calculated the same used for the last simulation environment.

The simulation results concerning the design and implementation of the low pass filters and complementary filters are presented in Fig. 4. The control system performance is evaluated resorting to a 5 centimeters settling time criteria, maximum relative error and the root mean square error, which results are presented in Table and II, III, and IV, receptively. It is duly noted the absence of overshoot for all the time constants. The settling time criteria assume that the relative position error settles for values less than 5 centimeters.

From the results presented, it can be concluded that the settling time regarding the relative position error varies proportionally with the time constant considered for in the design of the low pass filter. The root mean square error of the relative position error and its maximum relative error decreases with the increment of the time constant assumed in the tune of the low pass filter. The decrease of the root mean square error and maximum relative error, represents an improvement in the control system performance, however, it comes with an additional cost of increasing the settling time which is not desirable. Therefore, a compromise must be made concerning these properties. For further experimental implementation will

be considered a time constant $\alpha = 1$, since, for higher values, the system response starts to get to slow.

	Settling Time (s)						
	0	0.35	0.7	1	$\alpha = 1.35$	1.7	2
X Position	7.9	8.3	8.8	9.2	9.9	10.6	11.4
Y Position	8.9	9.1	9.5	10.0	10.6	11.1	11.8
Z Position	8.9	9.4	9.8	10.2	10.8	11.4	12.0

TABLE I: Front UAV Simulation Performance vs. α

	Settling Time (s)						
	0	0.35	0.7	1	1.35	1.7	2
X Position	9.3	9.7	10.1	10.5	10.9	11.6	11.9
Y Position	7.7	7.8	8.2	8.1	9.2	9.5	9.6
Z Position	11.12	11.5	12.0	12.3	12.8	13.39	13.8

TABLE II: Rear UAV Simulation Settling Time

	Maximum Relative Error (cm)						
	0	0.35	0.7	1	1.35	1.7	2
X Position	28.7	28.7	27.6	26.5	25.1	23.7	22.7
Y Position	19.8	20.8	18.9	17.9	18.1	16.1	14.8
Z Position	40.9	40.2	38.5	36.7	34.7	32.8	31.3

TABLE III: Rear UAV Simulation Maximum Relative Error

	Roar Mean Square Error (cm)						
	0	0.35	0.7	1	1.35	1.7	2
X Position	13.1	12.9	12.7	12.4	12.1	11.7	11.4
Y Position	8.3	8.3	8.0	7.8	7.6	7.4	7.4
Z Position	18.2	18.0	17.7	17.3	16.9	16.5	16.1

TABLE IV: Rear UAV Simulation Root Mean Square Error

VII. EXPERIMENTAL RESULTS

In this section, the analysis experimental results is presented alongside the implementation details.

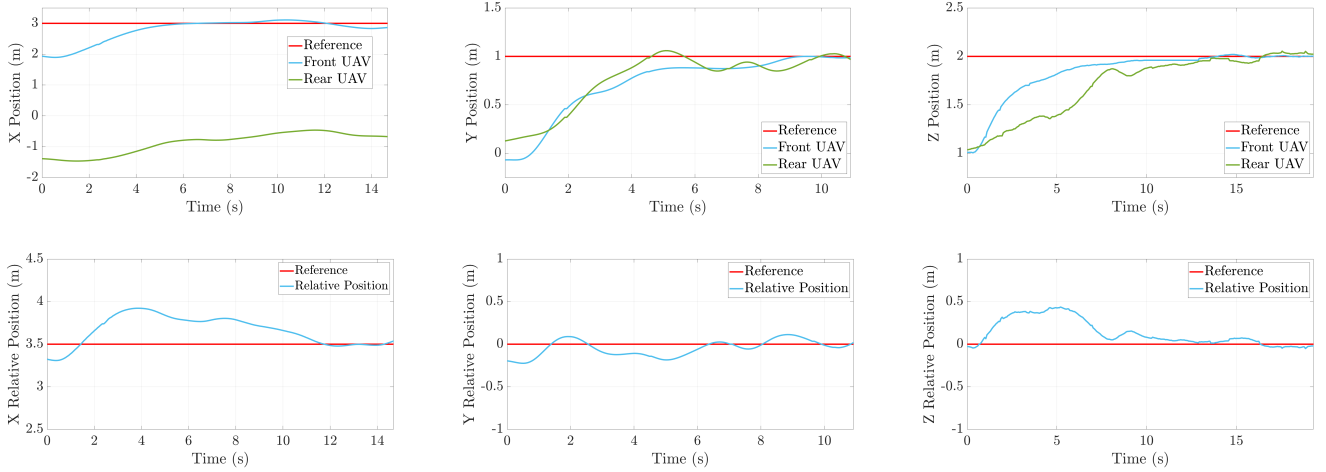


Fig. 5: Step-analysis Experimental results. From left to right, top to bottom: (a) X Position, (B) Y Position, (C) Z Position, (D) X Relative Position, (E) Y Relative Position, (F) Z Relative Position

A. Implementation

The implementation will be based on Parrot Ar.Drone 2.0. These quadrotors are controlled via WIFI in a range of 50 meters, having its own network defined as an access point. Parrot also provides a dedicated free app for the control of the quadrotor, live video streaming, making films and taking pictures.

In order to implement the control systems designed for the two UAVs, the AR Drone Simulink Development-Kit V1.1 (DevKit) provided in [11] is used. This Devkit provides simulink based models for the WIFI communication between both UAVs and a terminal, for instance, a personal computer. Here the control system is implemented in external mode. These simulink models allows sending combination of attitude (desired angles) and vertical speed commands as input control commands to the Ar.Drone embedded attitude inner control loop, and reading the states available upon the state reconstruction from the sensor data also built in the embedded electronics simultaneously. The state reconstruction provides estimations of the altitude, attitude angles, ground velocities.

For experimentally implement the control systems proposed, it is required to work in discrete time. The selected sample time for the controllers and filters meant to be implemented is 0.065 seconds, taking into consideration the slowest sensor built in the UAV, namely, the ultrasound which operates at a minimum sample time of 0.04 seconds. Therefore, the Qualisys system used as ground truth to the relative position and orientation is set to work also at a sample time of 0.065 seconds.

In order to reduce the ultrasound signal interferences between both UAVs, resulting in conflicts on the altitude estimation of both subsystems, one of the UAVs was set to operate at a different signal frequency. The reference distance along the longitudinal direction for the relative position was set to 3.5 meters.

The rear UAV, which is responsible for regulating the relative position, the controller was designed aiming a faster

response than the front UAV, in order to compensate more efficiently the delay present in the system.

B. Step Analysis

The LQR controller gains for the front and rear UAV, were calculated using the weighting matrices presented in table V and VI, and are presented in table VII and VIII.

In Figure 5 are presented the experimental results regarding the consequent unit step responses. Here, the unit step responses for the XYZ directions regarding the front UAV present a settling time (5%) is at 5.4, 5.6 and 8.9 seconds, respectively. The maximum overshoot is 3.8, 3.6 and 0 centimeters for the XYZ directions. The relative position between both UAVs along the XYZ directions settles at 6, 6 and 8 seconds, respectively. The maximum relative position errors between both UAVs along the XYZ directions is 35, 22, 43 centimeters, respectively. The control performance regarding the control of the relative position is presented in Table IX. For the evaluation of the performance is analyzed the settling time of the relative position regarding a 5 cm criteria mentioned before, maximum relative error and the root mean square error.

A video showing the cooperative load transportation reported in this thesis can be found in (<https://youtu.be/QIUf5pb1f1w>).

TABLE V: Front UAV LQR weighting matrices

	X Position	Y Position	Z Position
Q	$diag(3, 1, 1, 0)$	$diag(3, 1, 1, 0)$	$diag(3, 1)$
R	520	220	25

TABLE VI: Rear UAV LQR weighting matrices

	X Position	Y Position	Z Position
Q	$diag(3, 1, 1, 0)$	$diag(3, 1, 1, 0)$	$diag(3, 1)$
R	430	180	20

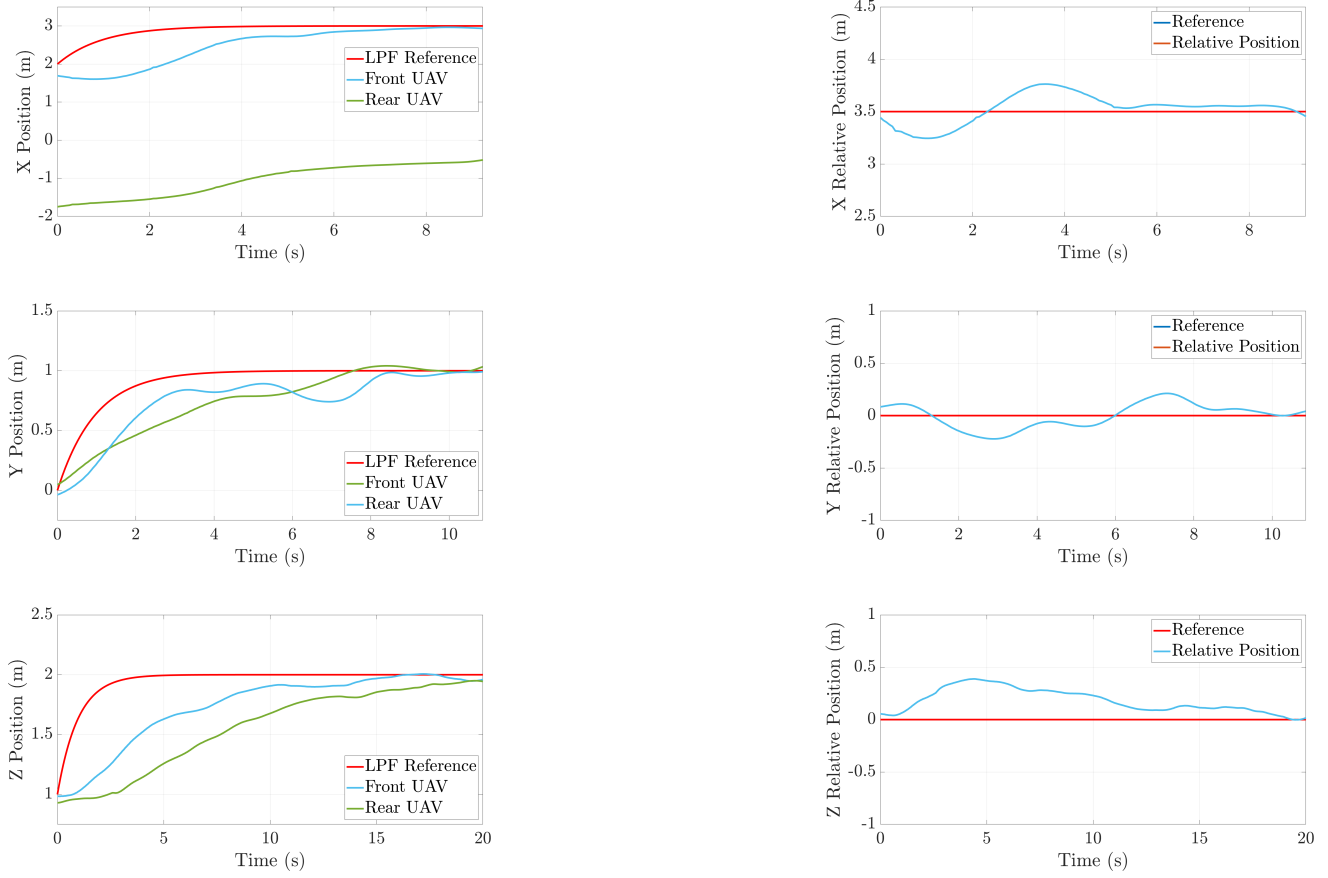


Fig. 6: Intermediary Filter Experimental results. From left to right, top to bottom: (a) X Position, (B) Y Position, (C) Z Position, (D) X Relative Position, (E) Y Relative Position, (F) Z Relative Position

TABLE VII: Front UAV Experimental LQR Gains

Gains	
X Position	$[-0.0753 \quad -0.0978 \quad 0.2009 \quad 0.0480]$
Y Position	$[0.1156 \quad 0.2323 \quad 0.0794 \quad 0.0156]$
Z Position	$[0.3425 \quad 0.0688]$

TABLE VIII: Rear UAV Experimental LQR Gains

Gains	
X Position	$[0.0828 \quad 0.1063 \quad -0.2183 \quad -0.0519]$
Y Position	$[-0.1277 \quad -0.2526 \quad -0.0870 \quad -0.0169]$
Z Position	$[-0.3823 \quad -0.0781]$

TABLE IX: Step Analysis- Rear UAV Experimental Performance

	Settling Time (5%)	Maximum Error	Root Mean Square Error
X Position	11 s	42.2 cm	23.29 cm
Y Position	6 s	22 cm	10.45 cm
Z Position	8 s	43 cm	20.25 cm

C. Intermediary Filters

In this section, is presented the experimental results regarding the implementation of the intermediary filter previously

described. Here, the relative position is still provided by a motion tracking system, upon which the rear UAV is capable of estimate the relative velocity. The results presented regarding the low pass filter tune performed in simulation, in order to improve the performance of the control system.

For the front UAV, the LQR controller gains are computed considering the state \mathbf{Q} and input \mathbf{R} weighting matrices presented in Table V, and are presented in Table VII. For the rear UAV, the LQR controller gains are computed considering the state and input weighting matrices presented in Table VI, and are shown in Table VIII. The experimental results concerning the design and implementation of the low pass filters and complementary filters are presented in Figure 6. Here, the results in the XYZ directions regarding the front UAV present a settling time (5%) is at 8.0, 10.5 and 10.0 seconds, respectively. The maximum overshoot is 0, 4.1 and 0.7 centimeters for the XYZ directions. The control system performance concerning the relative position is evaluated resorting to a 5 centimeters settling time criteria, maximum relative error and the root mean square error, which results are presented in Table X. The settling time criteria assume that the relative position error settles for values less than 5 centimeters.

For the X Position the prediction failed, where is noted a significant reduction to less than half of the settling time concerning the relative position error. This reduction can be justified by the demand for a response too aggressive for the control system designed for the rear UAV. Nevertheless, the implementation of the low pass filter restricted the frequency bandwidth of the system, resulting in lower frequency responses less demanding for the rear UAV to track, since the rear UAV actuators and control system present limited frequency bandwidth. This fact may also explain the slightly unexpected increase of the root mean square error, alongside the maximum relative error that remained equal.

TABLE X: Intermediary Filters- Rear UAV Experimental Performance

	Settling Time (5%)	Maximum Error	Root Mean Square Error
X Position	5 s	27.0 cm	14.19 cm
Y Position	8 s	22.0 cm	11.70 cm
Z Position	10 s	38.8 cm	19.39 cm

D. Position and Orientation Filter Results

In this section, is presented the experimental results concerning the implementation of the position and orientation filter presented previously. Here, the relative position and orientation are estimated resorting to rear UAV front camera. Therefore, the motion tracking system only is used to provide ground truth measurements, since all the estimation process is being done resorting only onboard sensors installed on the UAV. The position filter in use is designed only for estimations along the X and Y directions, thus only is presented the results regarding steps in these directions. The height is set to be constant during the experimental flights, being controlled resorting to altimeter measurements.

The front UAV integrates its ground velocities corrected by its yaw angle to estimate its position. Thus, since it is controlled the estimated position based only on optical flow measurements where noise is present, the position estimation gradually starts to drift.

Due to the UAV limitations in terms of payload carrying capacity, the target to be placed on the front UAV upon which is meant to estimate the relative position and orientation has to be relatively small. Thus, the camera was only able to take measurements on the target until a maximum relative distance of 4 m. However, since it meant to measure the movement of the front UAV, an abrupt maneuver may lead to the domain where the camera is not able to take measurements of the target. Therefore, the desired relative distance along the longitudinal direction X was set to 2.5 m instead of 3.5 m. This change leads to more accentuate altimeter inferences and air-flow cross disturbances, resulting in a poor performance of the control system. The altimeter inferences induce in poor measurements of the height directly influencing the optical flow measurements which resort to the estimation of the height.

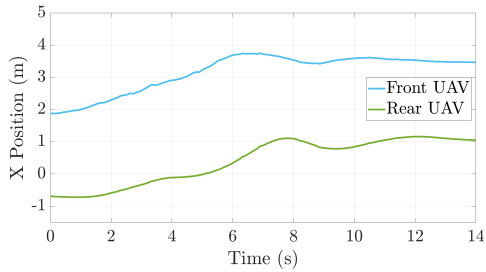
For the front UAV, the LQR controller gains are computed considering the state \mathbf{Q} and input \mathbf{R} weighting matrices presented in Table V, and are presented in Table VII. For the rear UAV, the LQR controller gains are computed considering the state and input weighting matrices presented in Table VI, and are shown in Table VIII. The experimental results concerning the design and implementation of the intermediary filters and position filter are presented in Figure 7. The control system performance is evaluated resorting to a 5 centimeters settling time criteria, maximum relative error and the root mean square error, which results are presented in Table XI. The settling time criteria assume that the relative position error settles for values less than 5 centimeters.

The results presented denotes very similar properties to the results presented in Fig. 6. Along the Y direction, the front UAV position settles at 10.2 s presenting an increase of 2.2 seconds, and the rear UAV settles the relative position at 9.0 seconds presenting a maximum relative position error of 22.6 cm and an increase of the root mean square error to 12.54 cm. Along the X direction, the front UAV position settles at 10.6 s presenting an increase of 2.2 seconds, and the rear UAV settles the relative position at 7.0 seconds presenting a maximum relative position error of 88.8 cm and an increase of the root mean square error to 34.78 cm.

The deterioration of the control performance is due the fact the control system is now only dependent on onboard sensors installed in the quadrotor, and because of the target of rectangular shape placed at the top of the front UAV concerning the estimation of the relative position and orientation. Since the target developed for this application presents a rectangular shape and is placed align with the front UAV referential frame, the inertial of the quadrotor gets compromised. This target has almost no thickness, presenting almost null variations on the inertial regarding the X direction which is directly related to the roll angles that governs the movement along the Y direction. However, the rectangular shape of the target induces a significantly increase of the inertial concerning the Y direction, resulting in a more accentuated poor control system performance when compared to the result presented in Fig. 6, since the pitch moment to be generated by the rotors has to be significantly higher. Nevertheless, the results presented in Fig.7 still prove the feasibility of the control system designed to perform the task, where the relative position converges presenting no steady-state error and satisfactory performances having in mind the assumptions done during the controllers design phase.

	Settling Time (5%)	Maximum Error	Root Mean Square Error
X Position	10.6 s	88.8 cm	34.78 cm
Y Position	9.0 s	22.6 cm	12.54 cm

TABLE XI: Position and Orientation Filer- Rear UAV Experimental Performance



(a) X Position

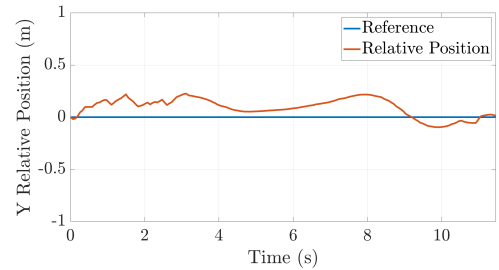
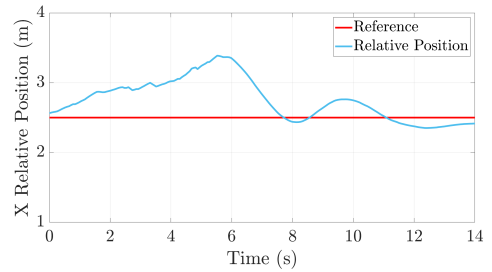
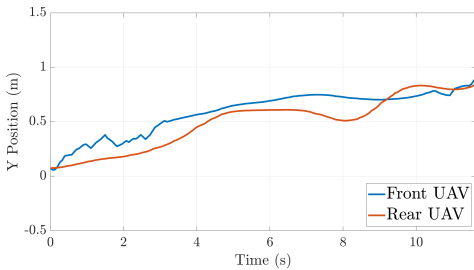


Fig. 7: Position and Orientation Filter Experimental results. From left to right, top to bottom: (a) X Position, (B) X Relative Position, (C) Y Position, (D) Y Relative Position

VIII. CONCLUSION

This thesis presents a methodology for cooperative load transportation by two quadrotors, given the state variables estimates, based on measurements from motion sensors installed onboard. The control and estimation solutions were required to ensure the stability of the system while guarantying a null steady-state position and estimation errors. The vertical velocity has to be estimated since there is no sensor usually onboard the quadrotors capable of providing this measurement directly.

Further, in order to turn the system independent of a motion tracking system to provide estimates of the relative position between the multiple UAVs, the UAVs, front camera is meant to be used in order to provide these estimates. Therefore, the relative velocity between the UAVs can be estimated upon these measurements.

The proposed solutions are presented based on linear control and estimation methods. These solutions include classical and optimal control and estimation theory. The controllers and estimators resort to linear and optimal control techniques, as the Linear Quadratic Regulators (LQRs) and Kalman filters, respectively.

The proposed control system is validated both in simulation and experimentally, resorting to a commercially available quadrotor equipped with an Inertial Measurement Unit (IMU), an ultrasound height, vertical and frontal cameras, among other sensors. The simulation environment models the noise present in the measurements provided by the sensors, as Gaussian white-noise for the experimental implementation of the control system proposed.

ACKNOWLEDGMENTS

This work was supported by FCT, through IDMEC, under LAETA, project UID/EMS/50022/2019

REFERENCES

- [1] R. M. Murray, "Trajectory generation for a towed cable system using differential flatness," in *IFAC world congress*, 1996, pp. 395–400.
- [2] S. Tang and V. Kumar, "Mixed integer quadratic program trajectory generation for a quadrotor with a cable-suspended payload," in *Robotics and Automation (ICRA), 2015 IEEE International Conference on*. IEEE, 2015, pp. 2216–2222.
- [3] P. Outeiro, C. Cardeira, and P. Oliveira, "Adaptive/multi-model height control system of a quadrotor constant unknown load transportation," in *2018 IEEE International Conference on Autonomous Robot Systems and Competitions (ICARSC)*, April 2018, pp. 65–70.
- [4] J. Fink, N. Michael, S. Kim, and V. Kumar, "Planning and control for cooperative manipulation and transportation with aerial robots," *The International Journal of Robotics Research*, vol. 30, no. 3, pp. 324–334, 2011.
- [5] K. Sreenath and V. Kumar, "Dynamics, control and planning for cooperative manipulation of payloads suspended by cables from multiple quadrotor robots," *m*, vol. 1, no. r2, p. r3, 2013.
- [6] K. Ogata, *Modern Control Engineering*, ser. Instrumentation and controls series. Prentice Hall, 2010.
- [7] *Qualisys*. [Online]. Available: <http://www.qualisys.com>.
- [8] V. K. R. Mahony and P. Corke, "Multirotor aerial vehicles: Modeling, estimation, and control of quadrotor," *Robotics Automation Magazine, IEEE*, vol. PP(99):1, 2012, iSSN 1070-9932. doi: 10.1109/MRA.2012.2206474.
- [9] M. Athans, "Derivation of the kalman-bucy filter using parameter optimization," MIT ISR/IST, Tech. Rep. KF #8A, 2001.
- [10] J. Madeiras, C. Cardeira, and P. Oliveira, "Complementary filter aided vision for attitude and position estimation: Design, analysis and experimental validation," in *21st IFAC Symposium on Automatic Control in Aerospace (ACA) 2019*, 08 2019.
- [11] D. Sanabria and P. Mosterman, "Ar drone simulink development-kit v1.1," November 2014, <https://www.mathworks.com/matlabcentral/fileexchange/43719>.